J|A|C|S
COMMUNICATIONS

Published on Web 09/09/2006

Efficient H_2 Adsorption by Nanopores of High-Purity Double-Walled Carbon Nanotubes

Junichi Miyamoto,[†] Yoshiyuki Hattori,[†] Daisuke Noguchi,[†] Hideki Tanaka,[‡] Tomonori Ohba,[†] Shigenori Utsumi,[†] Hirofumi Kanoh,[†] Yoong Ahm Kim,[§] Hiroyuki Muramatsu,[§] Takuya Hayashi,[§] Morinobu Endo,[§] and Katsumi Kaneko*,[†]

Department of Chemistry, Chiba University, Chiba, Japan 263-8521, Department of Chemical Engineering, Kyoto University, Nishikyo-ku, Kyoto, 615-8510 Japan, and Department of Electrical and Electronic Engineering, Shinshu University, Nagano, 380-8553 Japan

Received July 4, 2006; E-mail: kaneko@pchem2.s.chiba-u.ac.jp

Multiwalled carbon nanotubes (MWNTs)[1] and single-walled carbon nanotubes (SWNTs)[2,3] have stimulated nanoscale science and technology for electronic devices,[4,5] scanning microscopy probe tips,[6,7] and energy storage materials.[8] Also, carbon fibers which have nanotube structures produced by Endo et al. have been widely applied in technology.[9] SWNTs, in particular, have been actively studied, because of their greater uniformity of structure compared with that of MWNTs. Nevertheless, SWNTs still have issues with impurities such as amorphous carbon, metal catalysts, and carbon nanoparticles, although Hata et al. developed recently a highly sophisticated method of preparing SWNTs, resulting in greater than 99% purity.[10] Active studies on a SWNT have elucidated its unique properties, regardless of the presence of impurities. A comparison of a SWNT with a double-walled carbon nanotube (DWNT), which consists of two graphene layers, is required, because DWNTs are expected to have some advantages over SWNTs. DWNTs are much more stable than SWNTs[11] according to studies on nonuniform and impure DWNT samples. Recently, Endo et al. synthesized high-purity DWNT buckypaper with a catalytic chemical vapor deposition (CCVD) method using an optimized two-step purification process.[12,13] The newly prepared DWNT is extremely pure and uniform with only a trace amount of metal impurities and amorphous carbon. A comparative study of SWNTs and DWNTs using this high-purity DWNT is expected to result in a wide range of potential applications of nanocarbon. In this paper, we report that a highly ordered bundled structure of DWNTs can offer a much better adsorption field for H_2 than SWNTs.

In this study, we used DWNT samples synthesized with the CCVD method described by Endo et al.[12,13] A high-resolution TEM image of a DWNT shows the presence of an ordered-hexagonal-packed structure. To understand its gas adsorption properties, we needed to clarify the nanopore structure and the bundle structure using information on the primary DWNT particle from Raman spectroscopy, XRD measurements, and simulated H_2 adsorption isotherms.

We measured the Raman spectra with an Ar ion laser (514.5 nm). The Raman spectrum shows a weak D-band at 1353 cm^{-1} and a strong G-band peak. The band intensity of G-band to D-band, I(G)/I(D), shows that the DWNT sample has a highly ordered structure. The bands of radial-breathing-mode (RBM) of a DWNT indicate clearly the coexistence of inner and outer tubes. Analysis of the RBM bands indicated that this DWNT sample is a combination of two kinds of double wall tubes with inner and outer diameters of 0.72 and 1.48 nm and 0.91 and 1.61 nm, respectively.

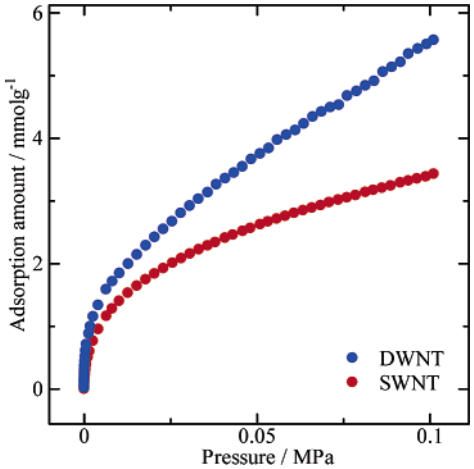

Figure 1. The H_2 adsorption isotherms of SWNTs and DWNTs at 77 K.

Table 1. Pore Structural Parameters Determined from the N_2 Adsorption Isotherms at 77 K on SWNTs and DWNTs

	BET SSA m^2g^{-1}	α_s-plot SSA m^2g^{-1}	micropore volume mlg^{-1}
SWNT	610	505	0.25
DWNT	330	320	0.17

We measured the N_2 adsorption isotherms of a DWNT and a SWNT at 77 K. The N_2 adsorption amount on the SWNT is much larger than that on the DWNT over the whole pressure range. The comparison plot of the N_2 adsorption amount on the DWNT against that on the SWNT is almost linear, indicating that the DWNT and SWNT adsorption sites for N_2 molecules resemble each other. We evaluated the specific surface areas (SSA) of both the SWNT and the DWNT from N_2 adsorption isotherms with the BET method and α_s-plot using the standard data of the Grand Canonical Monte Carlo (GCMC) simulated N_2 adsorption isotherm of the internal surface of a SWNT whose diameter is 8 nm.[14] The micropore volume was determined from a Dubinin−Radushkevich plot.[15] These surface parameters are summarized in Table 1. These results suggest that the SWNT has greater porosity than the DWNT.

Figure 1 shows adsorption isotherms of supercritical H_2 on a DWNT and a SWNT at 77 K. The DWNT can adsorb much more H_2 than the SWNT despite its 40% smaller specific surface area. To clarify the mechanism for H_2 adsorption in the DWNT bundle, we performed XRD measurements and GCMC simulation for H_2 adsorption at 77 K.

The SWNT has no strong XRD peak, whereas we can observe three explicit peaks at $2\theta = 1.95°$, 4.1°, and 11.8° for the DWNT.

[†] Chiba University.
[‡] Kyoto University.
[§] Shinshu University.

10.1021/ja064744+ CCC: $33.50

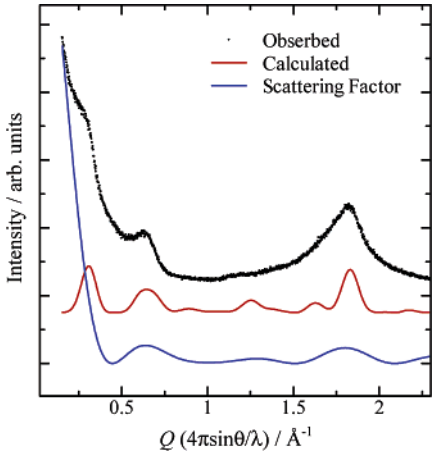

Figure 2. The calculated and observed XRD profiles of DWNT bundles.

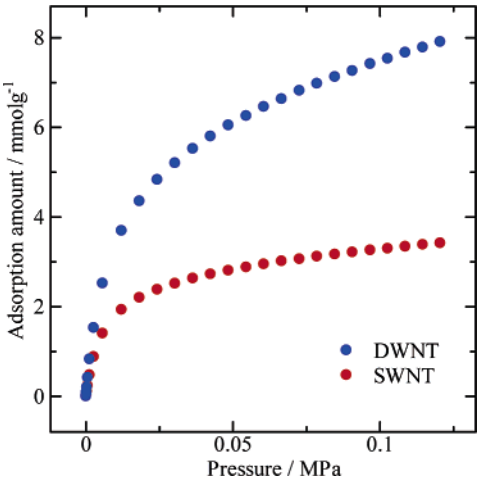

Figure 3. The simulated H_2 adsorption isotherms for DWNTs and SWNTs at 77 K.

The presence of three X-ray diffraction peaks for the DWNT indicates that the well ordered bundle structure has a two-dimensional triangular lattice. Therefore, the XRD profile with a triangular lattice was analyzed by use of the cylindrical Bessel function $J_0(\mathbf{Q}R)$ for the DWNT form factor, where $\mathbf{Q}$ and R denote the scattering vector and the carbon tube radius, respectively.[15] The calculated XRD profile for the DWNT was obtained using a model consisting of two concentric SWNTs. Thus, the DWNT form factor can be expressed as $F_C J_0(\mathbf{Q}R) + F_C J_0(\mathbf{Q}R')$, where R and R' denote the radii of the inner and outer tubes, respectively, and F_C is the atomic form factor of carbon atoms. Figure 2 shows the observed and calculated XRD patterns of the DWNT. The assumed parameters of the lattice constant, $a = 2.01$ nm, $R = 0.41$ nm, and $R' = 0.71$ nm, reproduce well the observed pattern. The van der Waals gap (g) for this model is 0.6 nm, which is double the gap in a perfect SWNT array. Although this DWNT has a well-ordered bundled structure from the TEM, RBM Raman bands, and the XRD, slight amount of tubes with other diameters should be present. Hence, the DWNT bundle is assumed to pack loosely into a hexagonal array and have interstitial pores which can adsorb H_2 molecules, even though they seem too small for the perfect accommodation of H_2 molecules. As the g value increases, the interstitial volume becomes larger but the molecular potential fields become weaker. Wang and Johnson reported that the optimal g value for a SWNT bundle is 0.6 nm.[17]

We performed GCMC simulations to study the adsorption of H_2 onto the DWNT (outer diameter equal to 1.43 nm and inner diameter equal to 0.77 nm)[11] bundle with $g = 0.6$ nm and the close-packed SWNT (diameter equal to 1.0 nm) bundle at 77 K. Figure 3 shows the simulated H_2 adsorption isotherms for the DWNT and the SWNT at 77 K. The DWNT bundle with wide g value can adsorb two times more H_2 than that of the close-packed SWNT bundle. The results also indicated that the interstitial sites were accessible by H_2 molecules and had a much deeper molecular potential field than that of a SWNT triangular array with $g = 0.6$ nm, owing to the overlapping of molecular potential from the double tube walls. This adsorbed state of H_2 in the interstitial sites of the DWNT was confirmed by a snapshot obtained with GCMC simulation. Thus, this DWNT bundle is well-suited for adsorption of H_2 molecules, adsorbing a larger amount than the SWNT, and hence adsorption fields with large adsorption capacities must be designed in the future.

Acknowledgment. This work is partially supported by a Grant-in-Aid for Fundamental Scientific Research (S) (Grant No. 15101003) and by the Evaluation of Hydrogen Storage on Nanocarbons, NEDO.

Supporting Information Available: Raman spectra, N_2 adsorption isotherms at 77 K, and H_2 adsorption isotherms at 77 K. This material is available free of charge via the Internet at http://pubs.acs.org.

References

(1) Iijima, S. *Nature* **1991**, *354*, 56.
(2) Iijima, S.; Ichihashi, T. *Nature* **1993**, *363*, 603.
(3) Bethune, D. S.; Klang, C. H.; De Vries, M. S.; Gorman, G.; Savoy, R.; Vasquez, J.; Beyers, R. *Nature* **1993**, *363*, 605.
(4) Tans, S. J.; Verschueren, A. R. M.; Dekker, C. *Nature* **1998**, *397*, 49.
(5) Bockrath, M.; Cobden, D. H.; McEuen, P. L.; Chopra, N. S.; Zettl, A.; Thess, A.; Smalley, R. E. *Science* **1997**, *275*, 1997.
(6) Dai, H.; Hafner, J. H.; Rinzler, A. G.; Colbert, D. T.; Smalley, R. E. *Nature* **1996**, *384*, 147.
(7) Nakayama, Y.; Nishijima, H.; Akita, S.; Hohmura, K. I.; Yoshimura, S. H.; Takeyasu, K. *J. Vac. Sci. Technol., B* **2000**, *18*, 661.
(8) An, K. H.; Kim, W. S.; Park, Y. S.; Moon, J.-M.; Bae, D. J,; Lim, S. C.; Lee, Y. S.; Lee, Y. H. *Adv. Funct. Mater.* **2001**, *11*, 387.
(9) Oberlin, A.; Endo, M.; Koyama, T. *J. Cryst. Growth* **1976**, *32*, 335.
(10) Hata, K.; Futaba, D. N.; Mizuno, K.; Namai, T.; Yumura, M.; Iijima, S. *Science* **2004**, *306*, 1362.
(11) Kim, Y. A.; Muramatsu, H.; Hayashi, T.; Endo, M.; Terrones, M.; Dresselhaus, M. S. *Chem. Phys. Lett.* **2004**, *398*, 87.
(12) Endo, M.; Muramatsu, H.; Hayashi, T.; Kim, Y. A.; Terrones, M.; Dresselhaus, M. S. *Nature* **2005**, *433*, 476.
(13) Muramatsu, H.; Hayashi, T.; Kim, Y. A.; Shimamoto, D.; Kim, Y. J.; Tantrakarn, K.; Endo, M. *Chem. Phys. Lett.* **2005**, *414*, 444.
(14) Ohba, T.; Kaneko, K. *J. Phys. Chem. B* **2002**, *106*, 7171.
(15) Dubinin, M. M. *Chem. Rev.* **1960**, *60*, 235.
(16) Thess, A.; Lee, R.; Nikolaev, P.; Dai, H.; Petit, P.; Robert, J.; Xu, C.; Lee, Y. H.; Kim, S. G.; Rinzler, A. G.; Colbert, D. T.; Scuseria, G. E.; Tománek, D.; Fischer, J. E.; Smalley, R. E. *Science* **1996**, *273*, 483.
(17) Wang, Q.; Johnson, J. K. *J. Phys. Chem. B* **1999**, *103*, 4809.

JA064744+